Mindos et al., https://doi.org/10.1083/jcb.201606052

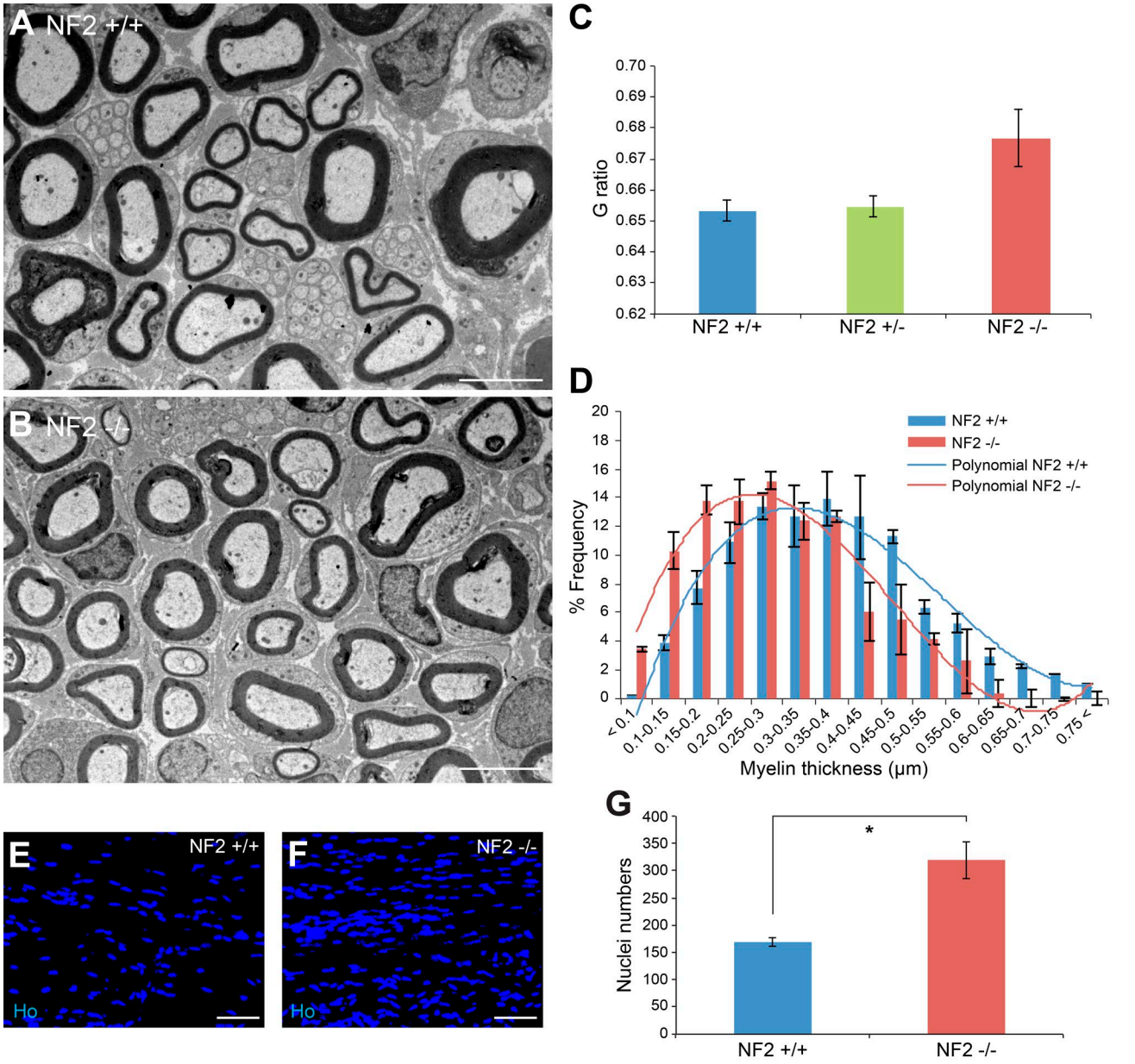

Figure S1. **Myelination and nuclei counts in nerves with SC-specific loss of Merlin.** (A and B) Transmission EM pictures of P21 control ($NF2^{+/+}$) and Merlin-null ($NF2^{-/-}$) nerves. Bars, 5 µm. (C) G ratio measurements of sciatic nerves from P21 control, Merlin heterozygous ($NF2^{+/-}$), and Merlin-null nerves. (D) Graph showing distribution of myelin thickness in P6 control and Merlin-null nerves. (A–D) $n = 3$ mice. (E–G) Hoechst-stained nuclei (E and F) and quantification (G) of longitudinal cryostat sections from adult intact sciatic nerves showing an increase in cell number in Merlin-null (F) nerves compared with control (E). Data are presented as means ± SEM. (E and F) $NF2^{+/+}$, $n = 3$ (E); $NF2^{-/-}$, $n = 5$ (F). Bars, 25 µm. (G) Two-sided two-sample Student's *t* test: *, P = 0.017.

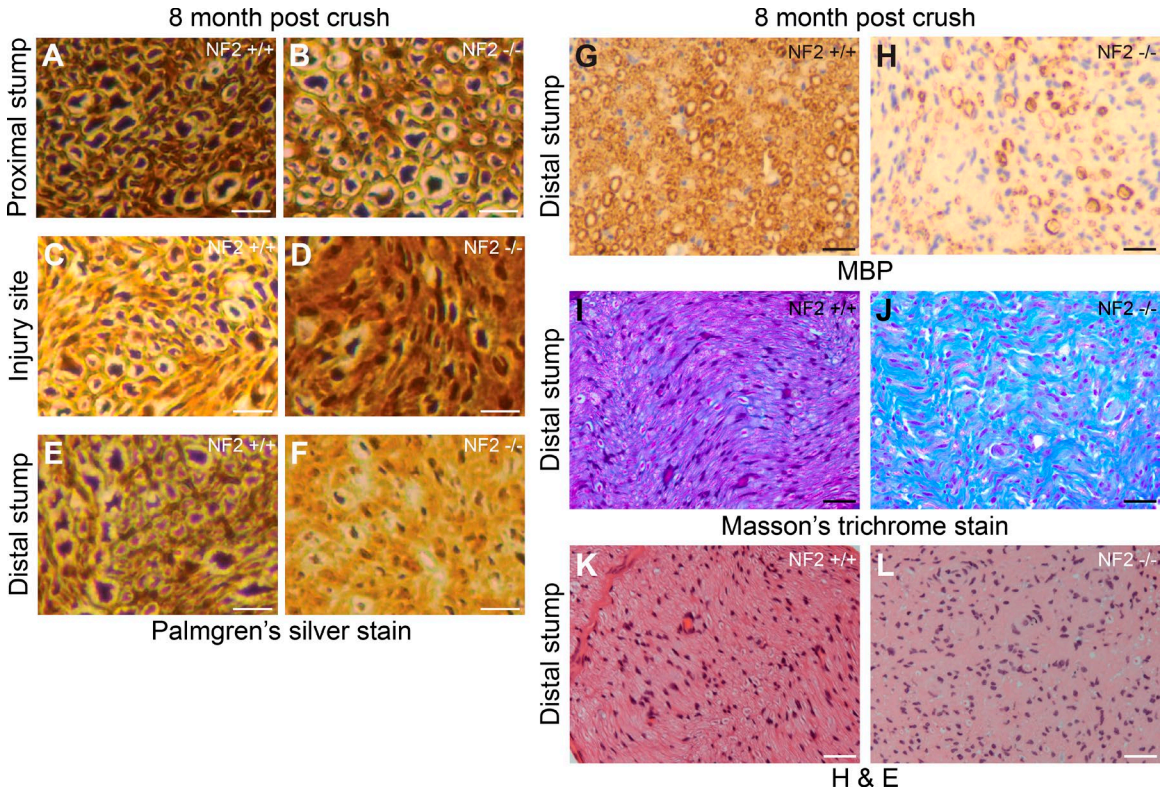

Figure S2. **Axonal regeneration, remyelination, and histology of control and Merlin-null nerves 8 mo after injury.** (A–F) Palmgren's silver stain showing axonal regeneration in control ($NF2^{+/+}$) and Merlin-null ($NF2^{-/-}$) nerves at 8 mo after crush injury. Sections of proximal nerve (A and B), injury site (C and D), and distal nerve (E and F) were stained to visualize axons with Palmgren's silver stain. Bars, 10 µm. (G and H) MBP immunolabeling of sections of the control (G) and Merlin-null (H) distal sciatic nerve showing low levels of MBP-positive remyelinated fibers in Merlin-null nerves at 8 mo after injury. (A–H) *n* = 6 mice. Bars, 50 µm. (I and J) Masson's trichrome stain showing collagen deposition (blue) in control (I) and Merlin-null (J) distal nerves at 8 mo after injury. Masson's trichrome staining colors the connective tissue blue and the cytoplasm red. Bars, 50 µm. (K and L) Hematoxylin and eosin (H&E) staining of control (K) and Merlin-null (L) distal nerves at 8 mo after injury. *n* = 6 mice. Bars, 50 µm.

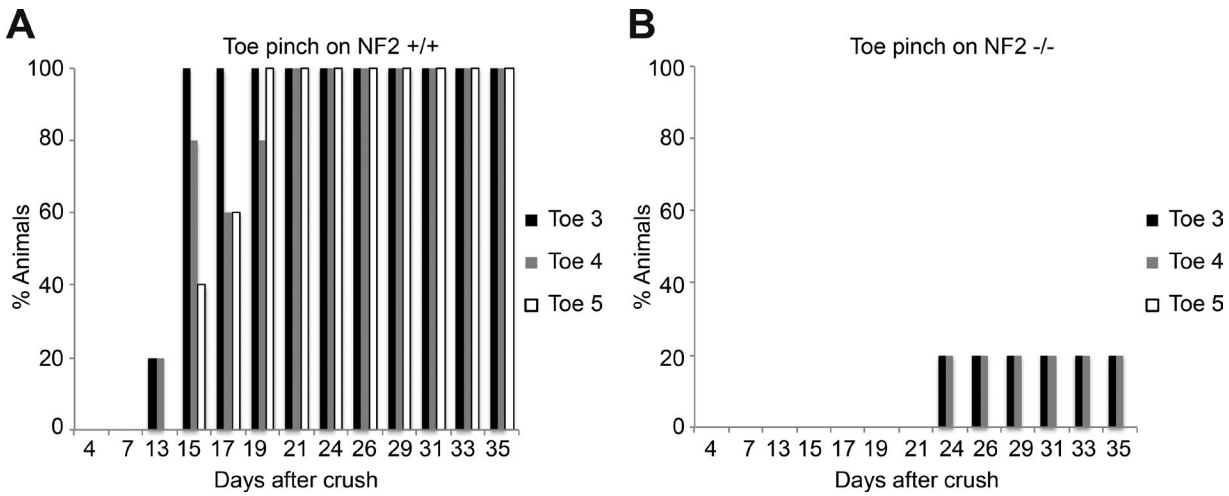

Figure S3. **Functional sensory testing of control and Merlin-null animals after crush injury.** (A and B) Graph of toe pinch data to measure sensory recovery at time points up to 35 d after injury for control ($NF2^{+/+}$) and Merlin-null ($NF2^{-/-}$) animals. Data are presented as means ± SEM. *n* = 5 mice.

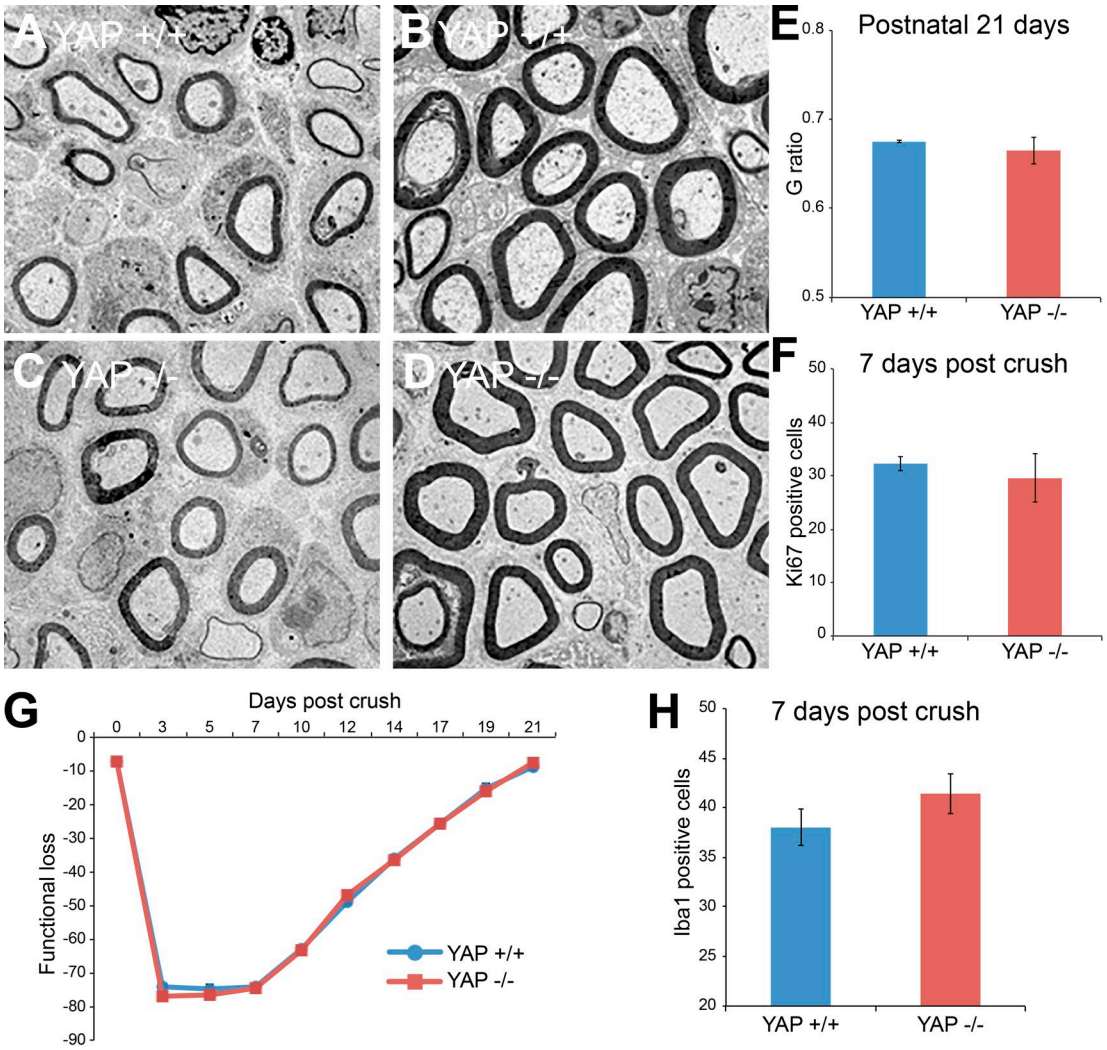

Figure S4. **Characterization of YAP single-null animals before and after injury.** (A–D) Transmission EM pictures of P6 (A and C) and P21 (B and D) sciatic nerves from control ($YAP^{+/+}$) and YAP-null ($YAP^{-/-}$) animals. (E) G ratio measurements of control and YAP-null animals at P21. *n* = 4 mice. (F) Counts of cell proliferation in distal nerves 7 d after nerve crush injury. (G) SSI measurements of control and YAP-null animals up to 21 d after nerve crush injury. (H) Numbers of Iba1-positive macrophages in the distal nerve at 7 d after nerve crush injury in control and YAP-null animals. Data are presented as means ± SEM. (F–H) *n* = 3 mice. (E–H) Two-sided two-sample Student's *t* test: P = 0.525 (E); P = 0.27 (F); P = 0.252 (H).

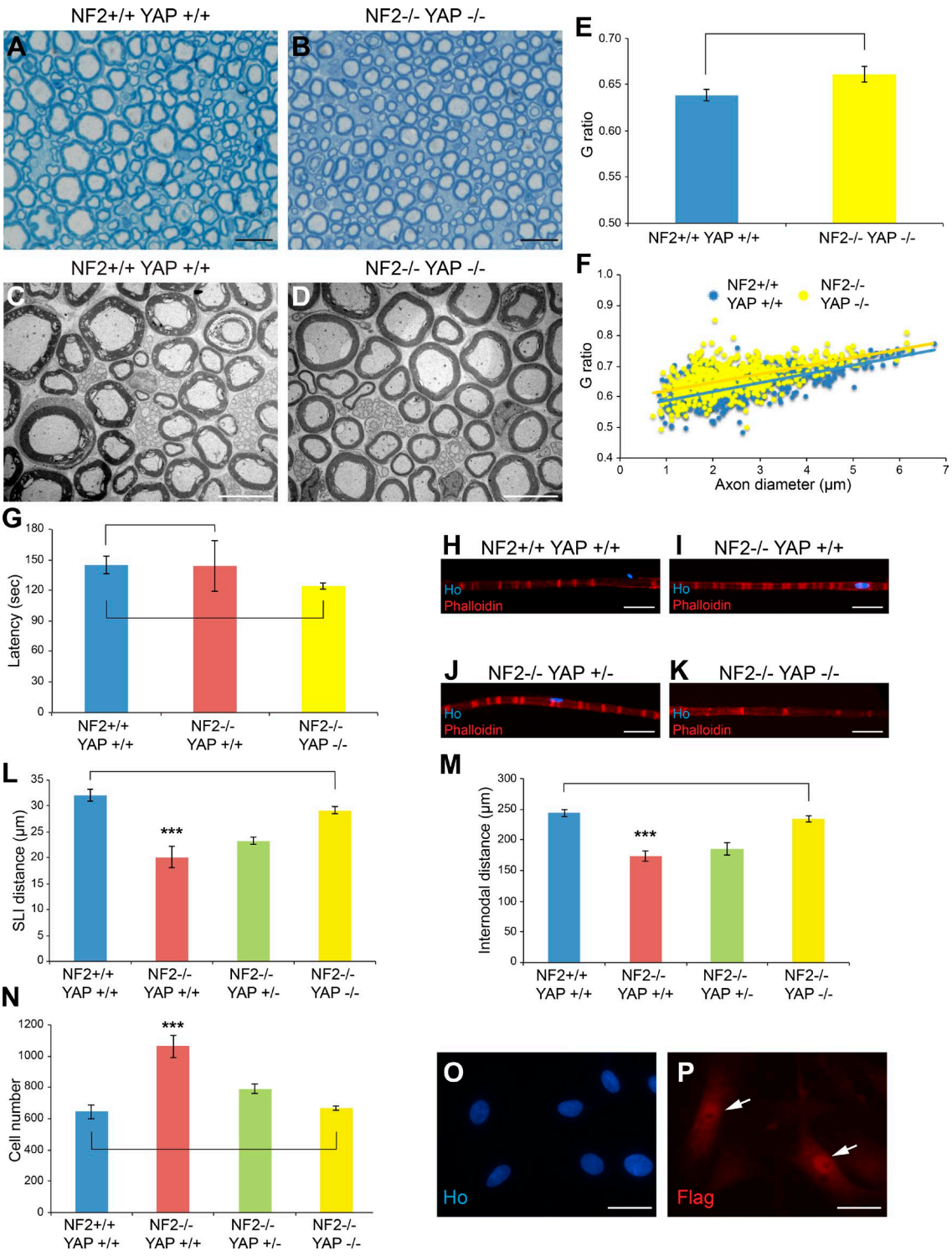

Figure S5. **Characterization of adult Merlin/YAP double-null sciatic nerves.** (A and B) Toluidine blue–stained semithin sections of adult control ($NF2^{+/+}YAP^{+/+}$) and Merlin/YAP double-null ($NF2^{-/-}YAP^{-/-}$) sciatic nerves. Bars, 10 µm. (C and D) Transmission EM images of adult control (C) and Merlin/YAP double-null (D) sciatic nerves. Bars, 5 µm. (E and F) G ratio measurements of control and Merlin/YAP-null nerves showing means (E) and scatter plots (F) of axon diameter versus G ratio. *n* = 3 mice per genotype. (G) Results of the rotarod test showing latency to fall on adult control, Merlin single-null, and Merlin/YAP double-null animals. (H–K) Phalloidin staining of teased nerve fibers of the sciatic nerve visualizing Schmidt-Lanterman incisures in control, Merlin single-null, and Merlin/YAP double-null adult nerves. Bars, 25 µm. (L–N) Loss of YAP in Merlin-null nerves normalizes the distance between adjacent Schmidt-Lanterman incisures (SLIs; L), internodal distance (M) in teased nerve fibers, and cell number (counts of Hoechst-stained nuclei in transverse cryostat sections; N) at P60. *n* = 4 mice. Data are presented as means ± SEM. (E and L–N) One-way analysis of variance with Bonferroni's multiple comparison test: *P* = 1 for $NF2^{-/-}YAP^{+/+}$ and P = 0.659 for $NF2^{-/-}YAP^{-/-}$ compared with $NF2^{+/+}YAP^{+/+}$ (E) and ***, $P \leq 0.001$ (L–N) for $NF2^{-/-}YAP^{+/+}$ compared with the other genotypes. P = 0.626 (L); P = 1 (M and N) for $NF2^{-/-}YAP^{-/-}$ compared with $NF2^{+/+}YAP^{+/+}$. (O and P) Hoechst (O) and Flag (P) immunolabeling of rat SCs expressing $YAP^{Ser127Ala}$. *n* = 3 experiments. Arrows in P indicate Flag-labeled YAP-overexpressing rat SCs showing clear cytoplasmic and nuclear localization of the $YAP^{Ser127Ala}$ protein. Bars, 10 µm. (E) Two-sided two-sample Student's *t* test: P = 0.103.